

PAPER • **OPEN ACCESS**

Backward facing step: from fluid flow to conjugate heat transfer with the coupling library preCICE

To cite this article: C G Caccia *et al* 2024 *IOP Conf. Ser.: Mater. Sci. Eng.* **1312** 012007

View the [article online](#) for updates and enhancements.

You may also like

- [Reynolds number effects on swirling flows intensity and reattachment length over a backward-facing step geometry using STD \$k\$ -turbulence model](#)
Steven Darmawan
- [Assessment of Turbulence Models on a Backward Facing Step Flow Using OpenFOAM®](#)
Anugya Singh, S Aravind, K Srinadhi *et al.*
- [Investigation of Subsonic and Hypersonic Rarefied Gas Flow over a Backward Facing Step](#)
Deepak Nabapure, Jayesh Sanwal, Sreeram Rajesh *et al.*



ECS The Electrochemical Society
Advancing solid state & electrochemical science & technology

ECS UNITED

247th ECS Meeting
Montréal, Canada
May 18-22, 2025
Palais des Congrès de Montréal

Showcase your science!

**Abstracts due
December
6th**

Backward facing step: from fluid flow to conjugate heat transfer with the coupling library preCICE

C G Caccia¹, M Corti², A Della Torre², and P Masarati¹

¹Politecnico di Milano, Milan, Italy, Department of Aerospace Science and Technology

²Politecnico di Milano, Milan, Italy, Department of Energy

E-mail: claudiogiovanni.caccia@polimi.it

Abstract. The Backward Facing Step geometry is a widely used benchmark problem in Computational Fluid Dynamics literature that is exploitable to validate models, solution methods, and software implementations. Despite a simple geometry, it shows phenomena like separation, reattachment, and re-circulation zones, under different flow conditions (i.e. different Reynolds number or turbulence parameters) it gives different measurable results, suitable for benchmarking activities [1]. Also regarding heat transfer analysis, the backward facing step can be used to investigate a wide variety of operating conditions (both for simple heat transfer cases and coupling heat transfer between the fluid region and a neighboring solid region giving rise to a more complex conjugate heat transfer model) [2]. This work uses the backward facing step as a test case to validate a numerical model built with the open-source Software OpenFOAM 10. The fluid and solid subdomains are connected through the open-source coupling library preCICE [3]. The results, taken from simulations carried out by the authors, show good agreement with the data available in the literature.

1. Introduction

The Backward Facing Step (BFS) geometry is a widely used benchmark problem in Computational Fluid Dynamics (CFD) literature to validate models, solution methods, and software implementations, mainly for the following reasons: despite a simple geometry, it shows separation, reattachment, and recirculation zones [4]; different flow conditions (i.e. different Reynolds numbers, Re) give different measurable results, suitable for benchmarking; heat flux from the lower wall can be used to investigate heat transfer characteristics; coupling heat transfer between the fluid region and a neighboring solid region gives rise to a conjugate heat transfer model. [5]

The BFS flow has the advantage of being described by a simple geometry and showing enough complexity to be considered as a test case. It is thus worth studying from many different points of view, based on the specific physics involved. Figure 1 shows a typical configuration of a backward facing step, introducing the main geometric parameters.

2. Objectives

The objectives of the present activity consist of generating a case within the OpenFOAM 10 framework for analyzing various aspects of the BFS model. Regarding fluid flow, we aim to evaluate the fluid model performance concerning pressure and velocity fields. Regarding heat transfer, we introduce in the model the energy equation, this stage is useful as an intermediary



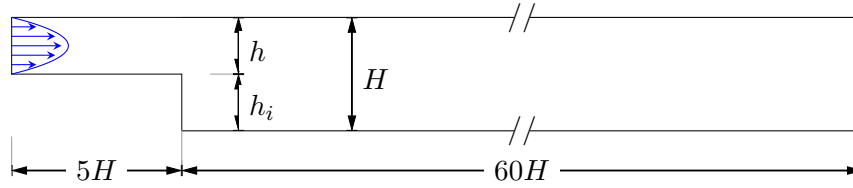


Figure 1. BFS geometry.

model, focusing on key heat transfer parameters. Regarding Conjugate Heat Transfer (CHT), we propose an integrated model consisting of a fluid region (validated in prior steps) and a solid region, where temperature fields and heat flux remain continuous at the interface. Throughout each stage, comparisons with existing literature data have been conducted to validate the findings.

3. Fluid flow simulations

Many studies have been conducted on the BFS. Considering an incompressible flow, the Reynolds number (based on the maximum channel height) is the driving parameter, and simulations range from $Re = 50$ to and over 80.000 [1].

In this study, we decided to focus, for the fluid flow analysis, on the case with:

$$Re_H = Re_{2h} = 800 \quad (1)$$

that is the case in which the step height is equal to the inlet height and the channel height ($h = h_i$ in Figure 1).

The CFD simulation is defined by a set of initial conditions encompassing geometric parameters and fluid properties, consolidated within a single configurable file. This file dictates geometric properties, mesh discretization, and essential fluid attributes such as velocity and viscosity calibrated to achieve a Reynolds number of $Re_H = 800$ (Equation 1).

A uniform mesh, generated using `blockMesh`, is employed, while boundary conditions are defined as follows: the inlet features a parabolic velocity profile, the outlet is set to uniform pressure and walls use a no-slip velocity condition.

Steady and incompressible analysis is conducted applying the `simpleFoam` solver, with velocity and pressure residuals set at 10^{-6} and 10^{-4} , respectively, to define the convergence of the simulation.

The results provided in various studies, such as [6], [7] and [5], allow assessing the fluid-dynamic quality of the model using the following parameters for comparison:

(i) Reattachment regions:

- $\frac{X_1}{h}$: first reattachment point on the lower wall
- $\frac{X_2}{h}$: first separation point on the upper wall
- $\frac{X_3}{h}$: first reattachment point on the upper wall

These regions are shown in Figure 3 and 4 for a better understanding.

(ii) Velocity and pressure profiles at section $\frac{X}{h} = 14$ and $\frac{X}{h} = 30$

The previous parameters have been used to perform a grid independence study.

The position of the separation and reattachment points (see Figures 3 and 4) is analyzed as a function of the mesh density, measured as the number of control volumes (CV) along h (volumes are square). The results are shown in Figure 5: all separation and reattachment points are within the benchmark region (see [7]) using a mesh with around 100 control volumes.

Data published in [6] allow to compare, once made non-dimensional, the values of the velocity and pressure profiles computed at different sections, in particular at $x = 14h$ and $x = 30h$. Figure 6 shows that the higher the control volumes, the closer the results are to the benchmark provided in [6]. Again, a number of control volumes around 100 looks to be enough to correctly describe the fluid flow.

4. Coupling with preCICE

The preCICE [3] software library¹, is an open-source tool designed to implement the connection of single-physics solvers, enabling the creation of partitioned multi-physics simulations such as fluid-structure interaction and conjugated heat transfer among others.

The simulations presented here involve the multiphysics coupling library preCICE [3], exploiting the adapter between preCICE and OpenFOAM [8].

Performing conjugate heat transfer (CHT) simulations using preCICE and OpenFOAM, rather than relying solely on `chtMultiRegionFoam`, offers several advantages. First, it provides better control over the coupling process between fluid and solid domains. This greater control facilitates the exploration of various coupling strategies and parameter settings, leading to improved accuracy and reliability in predicting heat transfer phenomena. Moreover, this allowed us to gain experience and insight into CHT parameters, fostering a deeper understanding of the underlying physics and computational techniques involved. Furthermore, the adoption of preCICE and OpenFOAM opens doors to future possibilities, such as coupling with other solid solvers, allowing to define different physical properties or to retrieve thermal stresses and deformations.

The preCICE coupling library enables communication between different physics solvers (in our case `rhoPimpleFoam` and `laplacianFoam`, as depicted in Figure 2). Its functionality extends to the definition of coupling strategies, with options like *loose* versus *tight* or *staggered* versus *parallel* approaches. Besides, preCICE allows the configuration of convergence methods and criteria, to improve the efficiency of coupled simulations. In case of non-conformal meshes at the interface of the domains, it is able to map data across disparate computational domains.

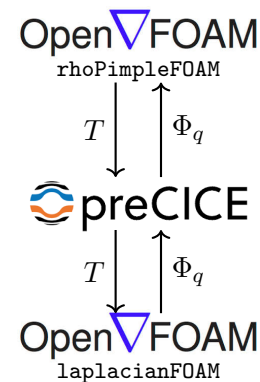


Figure 2. Coupling scheme.

¹ the code is accessible at the following repository: github.com/precice/precice

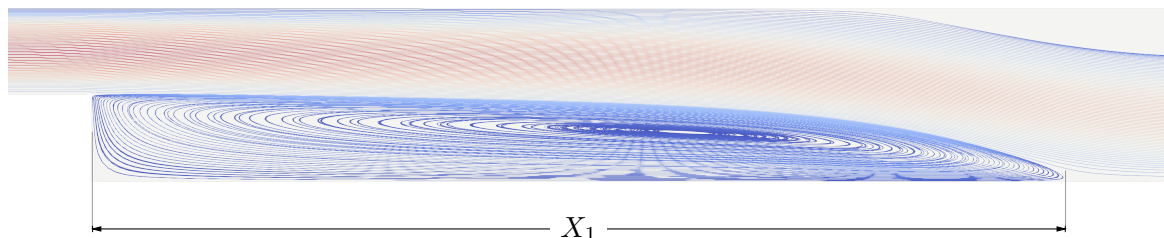


Figure 3. X_1 - first reattachment point.

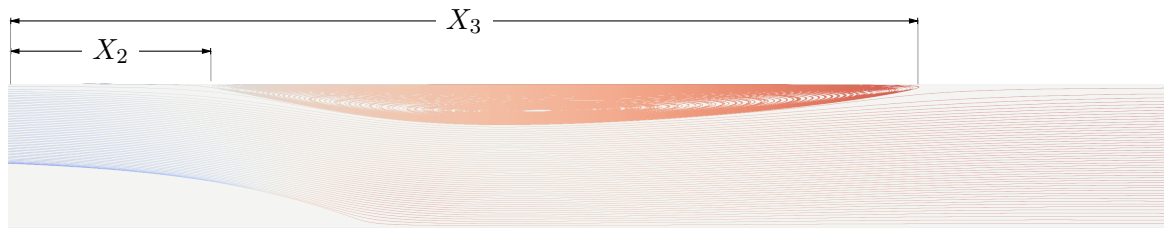


Figure 4. X_2 and X_3 - upper separation and reattachment points.

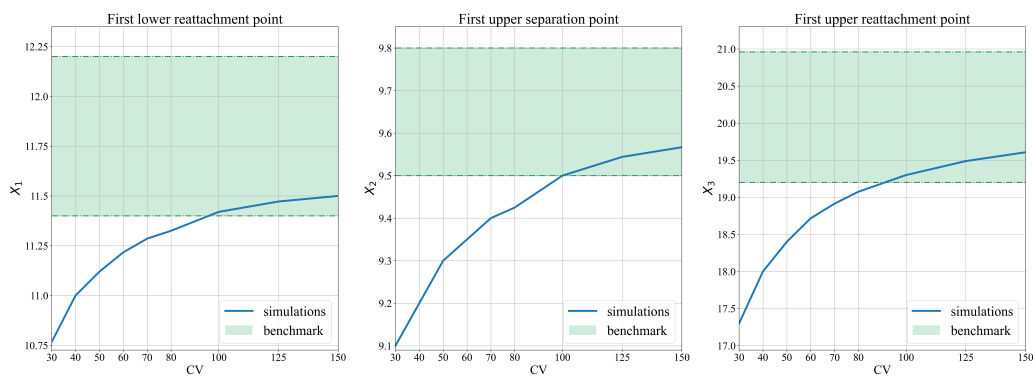


Figure 5. Separation and reattachment points.

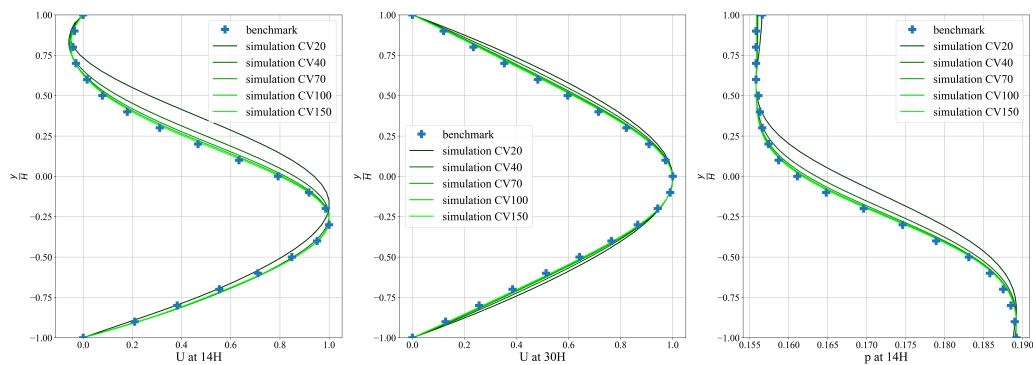


Figure 6. Velocity and pressure profiles.

5. Conjugate Heat Transfer simulations

The Conjugate Heat Transfer analysis stems from the fluid domain analyzed in Section 3 coupled with a solid domain. The two regions share a surface on which they exchange data (see Figure 7). The interface boundary conditions are expressed by the following equations:

$$T_s|_{interf} = T_f|_{interf} \quad (2)$$

$$k_s \frac{\partial T_s}{\partial y} \Big|_{interf} = -k_f \frac{\partial T_f}{\partial y} \Big|_{interf} \quad (3)$$

Equation 2 states that the temperature is continuous at the interface, while Equation 3 states that the heat flux exiting one region is equal to the heat flux entering the other region.

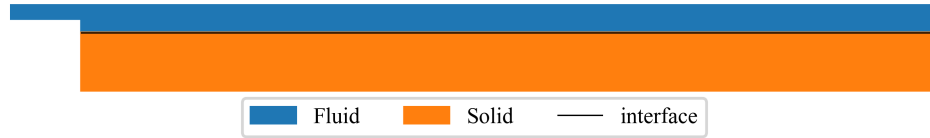


Figure 7. CHT domain.

5.1. Model Parameters

The CFD model has been built considering the following parameters:

Mesh

Same mesh for the fluid domain as previous cases, mesh for the solid domain connected to the lower part of the channel, with height $b = 4h$. Mesh defined using `blockMesh`.

Initial conditions

Fluid flow initialization as previous cases, solid initialized with uniform temperature T_{inlet} , while the lower wall of the solid is initialized with T_{lw} .

Fluid boundary and initial conditions

Same BCs as previous cases, in the domain *steady state* fluid solution and uniform temperature T_{inlet} .

Solid boundary and conditions

Imposed temperature T_{lw} at lower wall, adiabatic side walls, uniform temperature T_{inlet} in the domain.

Interface

Conditions expressed in Equation 2 and 3.

Solvers

`rhoPimpleFoam` and `laplacianFoam` with suitable Δt in order to have a reasonable *Courant number* in the fluid region and *diffusion* number in the solid region.

Physical Properties

- fluid region: $Re_H = 800$, $Pr = 0.71$, density $\rho = const$
- solid region: thermal conductivity k_S such that $k_{ratio} = \frac{k_S}{k_F} = [1, 10, 100, 1000]$.

5.2. Benchmark data

The data available in the literature (see [4] and [5]) to check the quality of the solution are the temperature distribution in the two regions at defined sections ($\frac{x}{H} = 6, 14, 30$), the temperature profile and the Nusselt number along the interface.

The local Nusselt number is defined as follows:

$$Nu(x) = - \left. \frac{\partial \theta}{\partial n} \right|_{interf} \quad (4)$$

where θ is the dimensionless temperature, defined as $\theta = \frac{T - T_{inlet}}{T_{lw} - T_{inlet}}$

6. Results

We performed transient simulations on temperature starting from the fully developed fluid flow to assess the temperature evolution in the fluid and in the solid, upon reaching a steady state. We measured the temperature evolution at 4 watchpoints on the interface, as shown in Figure 8. Figure 9 shows the evolution of the temperature at different values of k_{ratio} , which affects the final temperature at watchpoints and the time required to reach a steady state condition.

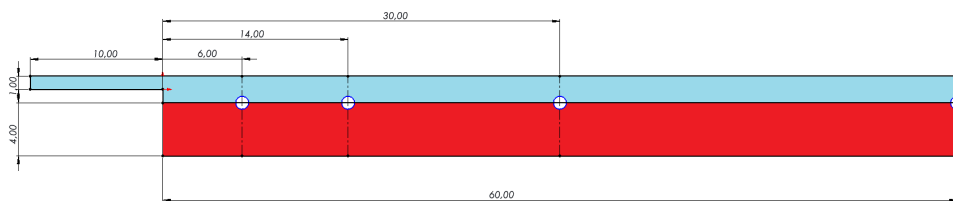


Figure 8. Watch-points.

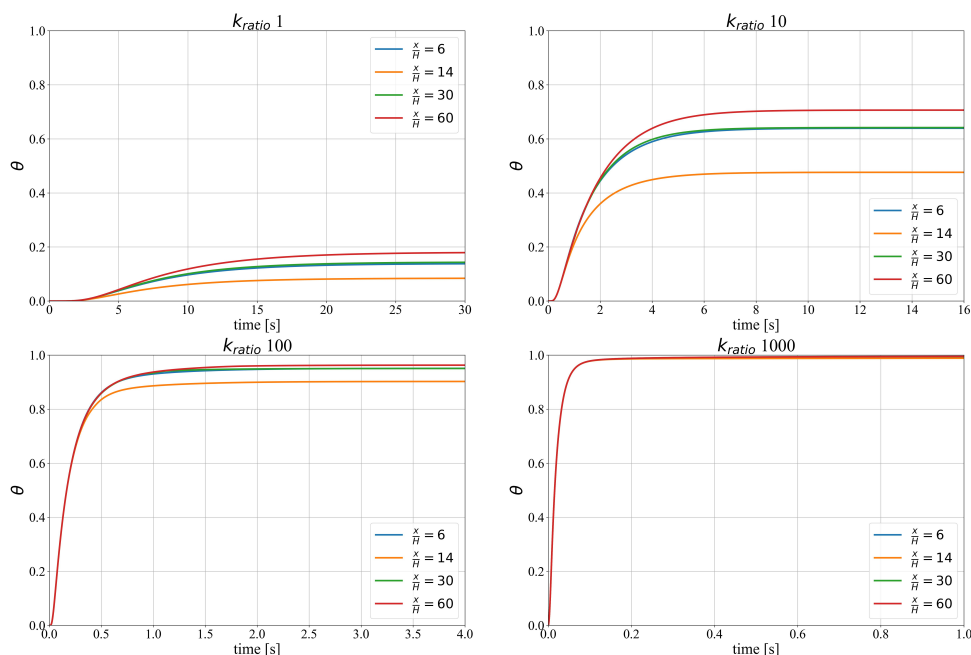


Figure 9. Temperature distribution.

6.1. Temperature profiles on sections

Figures 10 and 11 show the temperature profiles, taken at different positions, for the numerical case compared with the benchmark data. The temperature profiles look identical to the benchmark. The strong coupling imposed in the simulations looks to guarantee the expected solution. It's possible to notice that the continuity of the solution between the solid and the fluid domain is ensured.

6.2. Temperature and Nusselt number profiles at interface

Figures 12 and 13 show the temperature profiles, taken at the interface, for the numerical case solutions compared with the benchmark data. Similarly to the previous results, in each figure the value of the k_{ratio} parameters changes between the proposed values. Only the cases with $k_{ratio} = 1, 10$ are shown.

The graphs regarding the temperature along the interface confirm good agreement with the benchmark, although the lowest temperature position and value is slightly underestimated, in particular for $k_{ratio} = 100$. The Nusselt number (expression of the heat flux at the interface), shown in Figures 14 and 15, is very close to the benchmark, apart from the peak region corresponding to the recirculation zone, where the temperature is slightly underestimated.

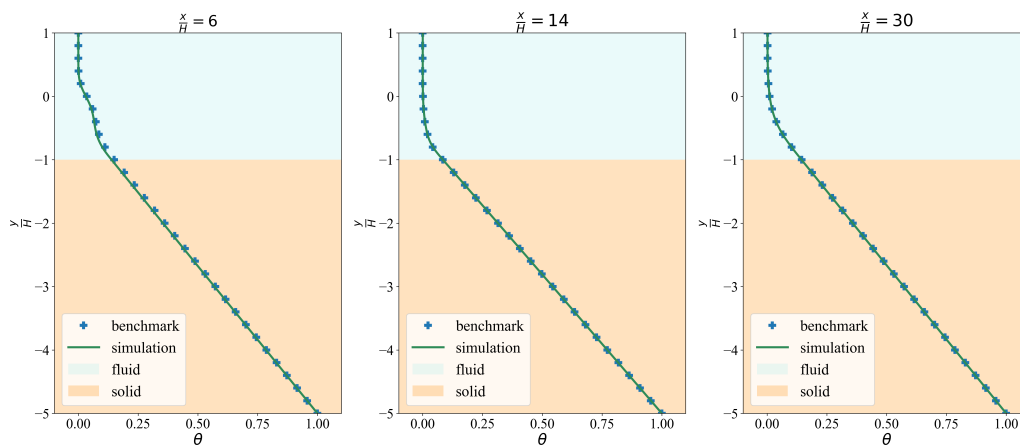


Figure 10. Temperature profile for $k_{ratio} = 1$.

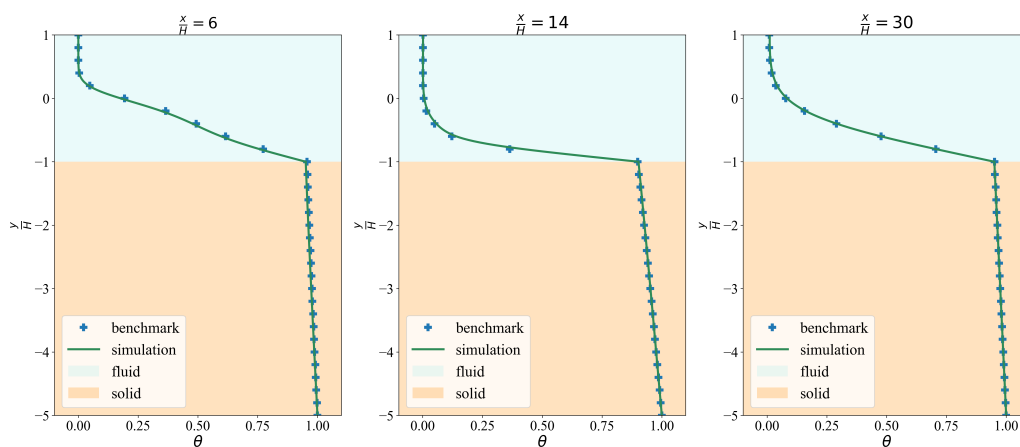


Figure 11. Temperature profile for $k_{ratio} = 100$.

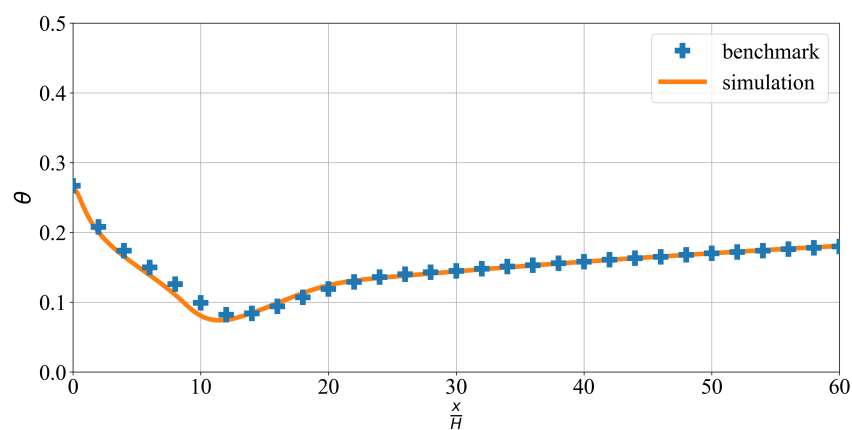


Figure 12. Temperature along interface for $k_{ratio} = 1$.

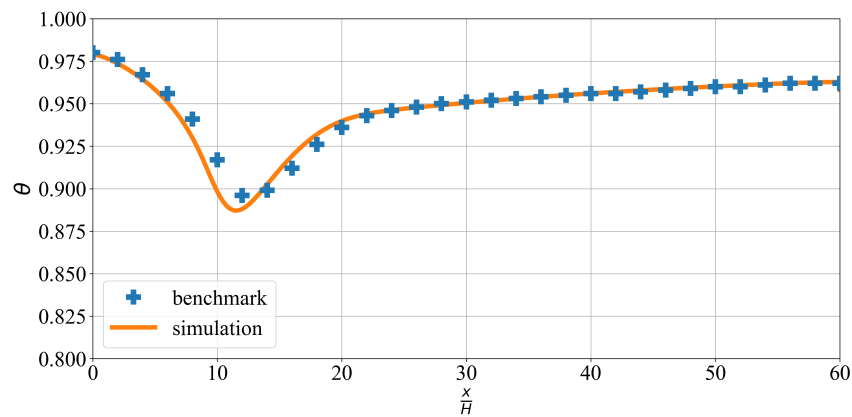


Figure 13. Temperature along interface for $k_{ratio} = 100$.

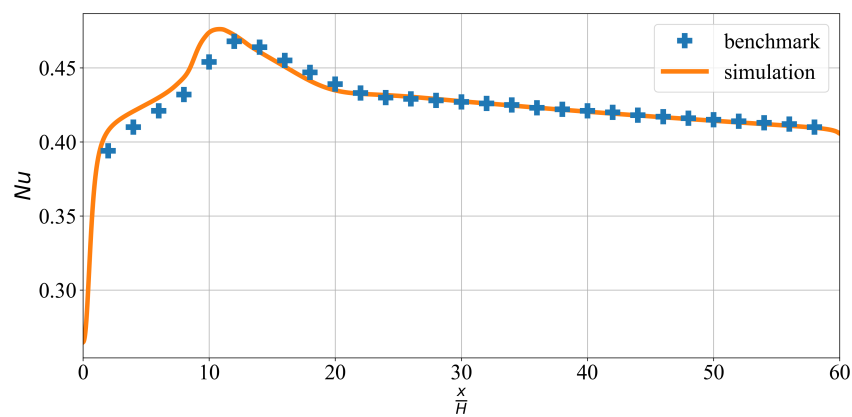


Figure 14. Nusselt number along interface for $k_{ratio} = 1$.

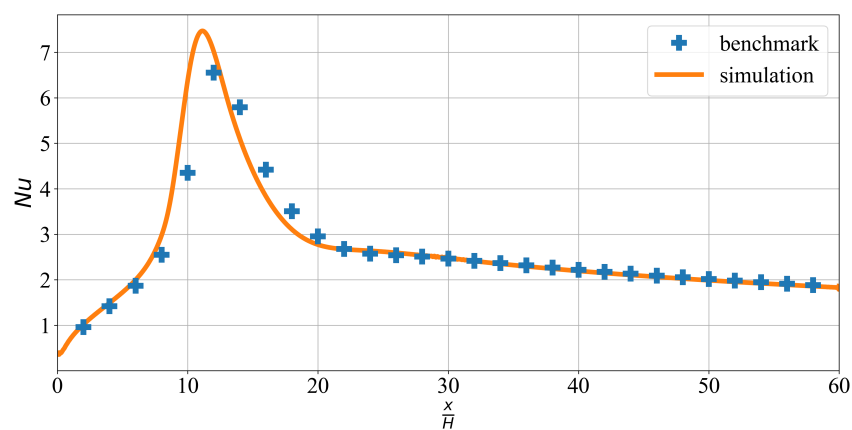


Figure 15. Nusselt number along interface for $k_{ratio} = 100$.

6.3. Coupling parameters

The coupling model concerns the way the solvers are interconnected and how convergence is reached. The configuration for our simulations, defined in preCICE, considers:

- *strong coupling*: that is, each time-step is iterated until convergence is reached,

- *staggered simulation*: rhoPimpleFoam is executed first, laplacianFoam second,
- *Aitken* under-relaxation [9]: other more complex acceleration proved no better,
- *residual control*: relative measure $1 \cdot 10^{-4}$ on temperature and heat flux.

the parameter k_{ratio} impacted the average number of iterations required to reach convergence, as shown in Table 1:

Table 1. Average coupling iterations.

k_{ratio}	1	10	100	1000
avg. iterations	1.389	2.871	6.910	21.216

7. Conclusions

In this proposed analysis, different aspects concerning fluid flow and heat transfer in a BFS geometry have been validated. For the fluid-dynamics aspects, the focus has been on a chosen Reynolds number ($Re_H = 800$), in which the flow is laminar but close to transition. A relationship between the mesh fineness and the main separation and reattachment points of the flow have been studied. The analysed characteristics have been the reattachment regions and velocity and pressure profiles. All the considered parameters show good agreement with literature data.

For the conjugate heat transfer analysis a model consisting in a solid domain attached to the lower wall of the channel has been considered. In particular, the temperature distribution in the solid and in the fluid regions as a function of the ratio between the fluid and the solid thermal conductivity have been analyzed. All models have been created using different OpenFOAM solvers connected through the coupling library preCICE.

All simulations showed satisfactory agreement between numerical results and the benchmarks data available in literature.

The BFS geometry, despite its simplicity, confirms to be an affordable candidate to validate models ranging from pure CFD to more complex multiphysics models like CHT.

Availability of data and materials

The dataset and the materials used for the study described in this article is available upon request to the authors.

References

- [1] Chen L, Asai K, Nonomura T, Xi G and Liu T 2018 *Therm. Sci. Eng. Prog.* **6** 194–216
- [2] Kanna P R and Das M K 2006 *Int. J. heat mass transf.* **49** 3929–3941
- [3] Chourdakis G, Davis K, Rodenberg B, Schulte M, Simonis F, Uekermann B, Abrams G, Bungartz H, Cheung Yau L, Desai I, Eder K, Hertrich R, Lindner F, Rusch A, Sashko D, Schneider D, Totounferoush A, Volland D, Vollmer P and Koseomur O 2022 *Open Research Europe* **2** URL <https://doi.org/10.12688/openreseurope.14445.2>
- [4] Kanna P R and Das M K 2009 *J Heat Transfer.* **131**
- [5] Ramšak M 2015 *Int. J. heat mass transf.* **84** 791–799
- [6] Gartling D K 1990 *Int J Numer Methods Fluids.* **11** 953–967
- [7] Teruel F E and Fogliatto E 2013 *Mecánica Computacional* **32** 3265–3278
- [8] Chourdakis G, Schneider D and Uekermann B 2023 *OpenFOAM® Journal* **3** 1–25 URL <https://journal.openfoam.com/index.php/ofj/article/view/88>
- [9] Irons B M and Tuck R C 1969 *International Journal for Numerical Methods in Engineering* **1** 275–277